A Study of the Role of Plant Properties in Arm Trajectory Formation

Lina L.E. Massone and **Jennifer D. Myers**

Technical Report 2/94
Neural Information Processing Laboratory
Northwestern University

Lina L.E. Massone (massone@eecs.nwu.edu) is with the Department of Electrical Engineering & Computer Science and the Biomedical Engineering Department of Northwestern University, 2145 Sheridan Road, Evanston, IL 60208-3118.

Jennifer D. Myers (jmyers@eecs.nwu.edu) is with the Institute for Neuroscience of Northwestern University, 2153 North Campus Drive, Evanston, IL 60208-3520.

Submitted July 1994 to *IEEE Transactions on Systems, Man, and Cybernetics.*

Abstract

This paper describes the response of a neural-network model of an anthropomorphic arm to various patterns of activation of the arm muscles. The arm model was introduced and described in detail in [1]. The purpose of the simulation experiments presented here is to study the relative role of control strategies and plant properties in trajectory formation, namely which features of simple arm movements can be attributed to the properties of the plant alone – a study that might provide some guidelines for the design of artificial arms. Our simulations demonstrate the performance of the model at steady-state, what movements the model produces in response to various activations of its muscles, and the generalization abilities of the recurrent neural network that implements the forward dynamic transformation. The results of our simulations emphasize the role of the intrinsic properties of the plant in generating movements with anthropomorphic qualities such as smoothness and unimodal velocity profiles and demonstrate that the task of an eventual controller for such an arm could be simply that of programming the amplitudes and durations of steps of neural input without considering additional motor details. Our findings are relevant to the design of artificial arms and, with some caveats, to the study of brain strategies in the arm motor system.

1 Introduction

In this paper we describe the response of a biologically-inspired neural-network model of an arm to various patterns of activation of its muscles. The details of the model and its rationale were amply described in [1]. In the following we will briefly summarize the overall model organization. We modeled the arm with two joints (shoulder and elbow) and six muscle-like actuators: two antagonist actuators that act across the shoulder joint (shoulder muscles), two antagonist actuators that act across the elbow joint (elbow muscles) and two antagonist actuators that act across both the shoulder and the elbow joints (double-joint muscles). The arm moved in the horizontal plane subject to the action of gravity. The overall transformation that the neural-network model computes is the transformation between the control signals that activate the six muscles (that in [1] we called "neural inputs" in analogy with the biological system) and the coordinates of the arm endpoint. This transformation is composed of four interacting stages (see Figure 1):

(1) The muscles are activated by their neural inputs, $\underline{ni}$, and they produce torques, $\underline{\tau_m}$, as functions of the neural inputs, the angular positions, $\underline{\theta}$, and the angular velocities, $\underline{\dot{\theta}}$.

(2) The muscles torques are combined into joint torques, $\underline{\tau}$, according to geometric principles.

(3) The forward dynamic block computes the angular accelerations, $\underline{\ddot{\theta}}$, as functions of the current values of $\underline{\tau}, \underline{\theta}$ and $\underline{\dot{\theta}}$. The resulting accelerations are then integrated to yield the new values of $\underline{\theta}$ and $\underline{\dot{\theta}}$.

(4) The forward kinematic block transforms the angular coordinates into coordinates of the endpoint, $\underline{x}$.

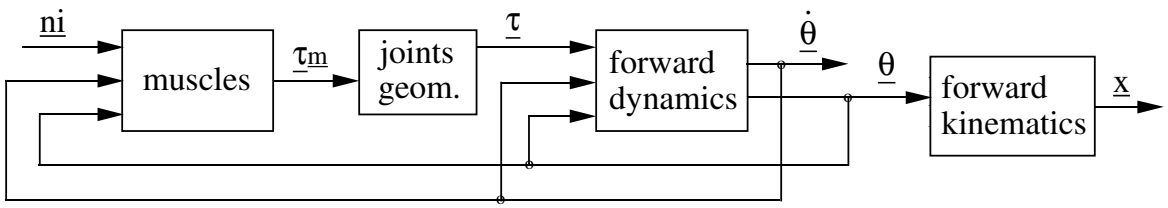

Figure 1: Architecture of the arm model.

The various stages interact with each other through a number of recurrent connections. We modeled each stage with feedforward and recurrent networks. For stage (1) we utilized six recurrent networks, one for each muscle. We derived the architecture and weights for such networks from the equations that describe the action of an elastic actuator according to a linearized version of the Hill's model [2]. For stage (2) we utilized a linear feedforward network that implemented simple geometrical constraints at the joints. Stage (3) consisted of training a nonlinear recurrent network to compute the forward dynamics of the arm. Finally, we implemented stage (4) with a feedforward nonlinear network, whose architecture and weights were derived from the equations of the forward kinematics of the arm. In [1] we also described a possible initialization procedure, that positions the arm as shown in Figure 2a. The chosen (and not unique) values of the six neural inputs for that arm position are shown in Figure 2b.

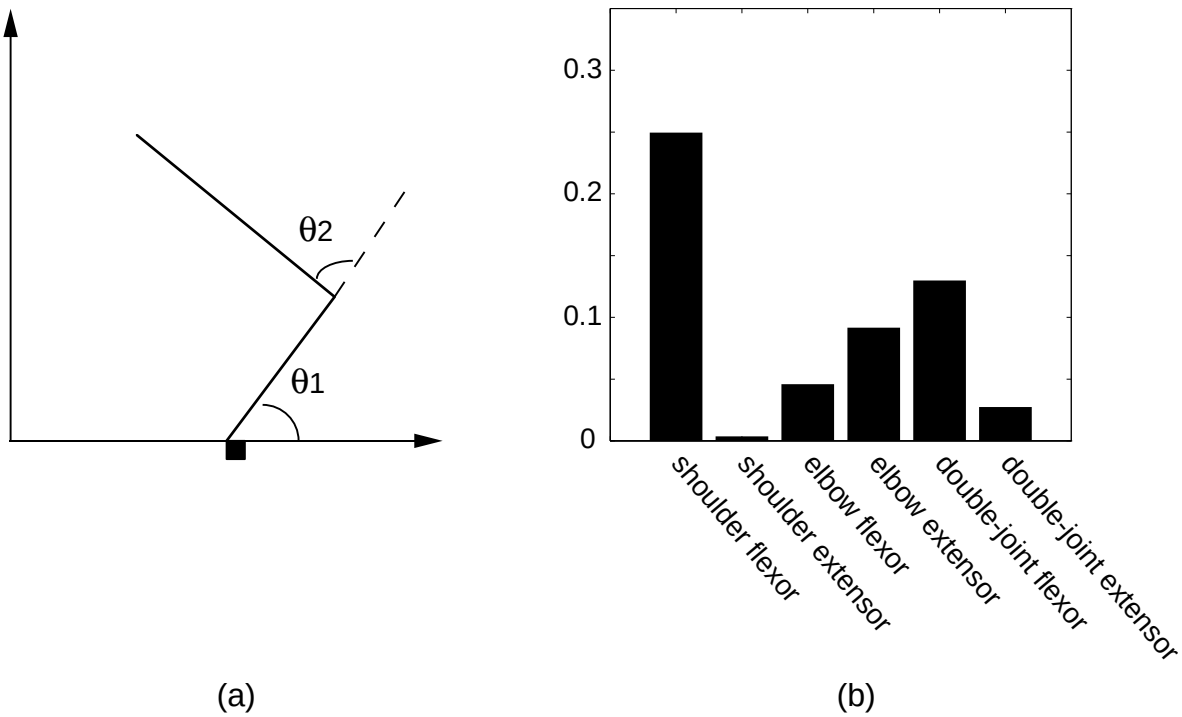

Figure 2: (a) The initial arm posture. (b) One of the possible configurations of neural inputs that holds the arm in the posture shown in Figure 2(a).

These values represent the initial configuration of neural inputs that we utilized for all the simulations described in this paper. We also experimented with different configurations and we did not observe macroscopic differences in the overall behavior of the arm. Another parameter of the arm model that must be chosen is the sampling step, Δt. In all our simulations we used a value of Δt equal to 5 $msec$. However, this is by no means a binding choice, as pointed out in [1].

In the following sections we demonstrate how our model responds to various patterns of neural input and we analyze the resulting, unpredictable movements of the arm endpoint. For the patterns of neural input we chose steps with random amplitudes and durations. The purpose of this study is to assess to what extent the plant properties play a role in determining basic kinematic aspects of arm movements such as smoothness and bell-shaped velocity profiles. The idea that biomechanics is an important component of human movement has been pursued in a number of studies, e.g. [3], [4], [5], [6], [7], [8]. The contribution of our study to this issue is that of providing an extended analysis of the response of a complicated, multijoint device to random activations of its actuators, and that of pointing out what insights one can gain, from the results of such experiments, at the level of eventual control strategies. Our study is significant in two respects. From an engineering perspective it demonstrates that it is advantageous to build artificial arms based on the properties of the human arm. From a biological standpoint it sets some ground for further explorations of the control strategies of the central nervous system.

2 Simulation Results

2.1 Stability

In the first simulation experiment we demonstrate the stability of our system. We activated the six muscle-like actuators with constant levels of neural input corresponding to the equilibrium values shown in Figure 2b. If our model was error-free then those levels of neural input would keep the arm perfectly in place in the configuration of Figure 2a. However the response of the forward dynamic network (see Figure 3) is not error-free due to the residual errors of the training procedure. Such errors are also likely to be amplified by the cascaded

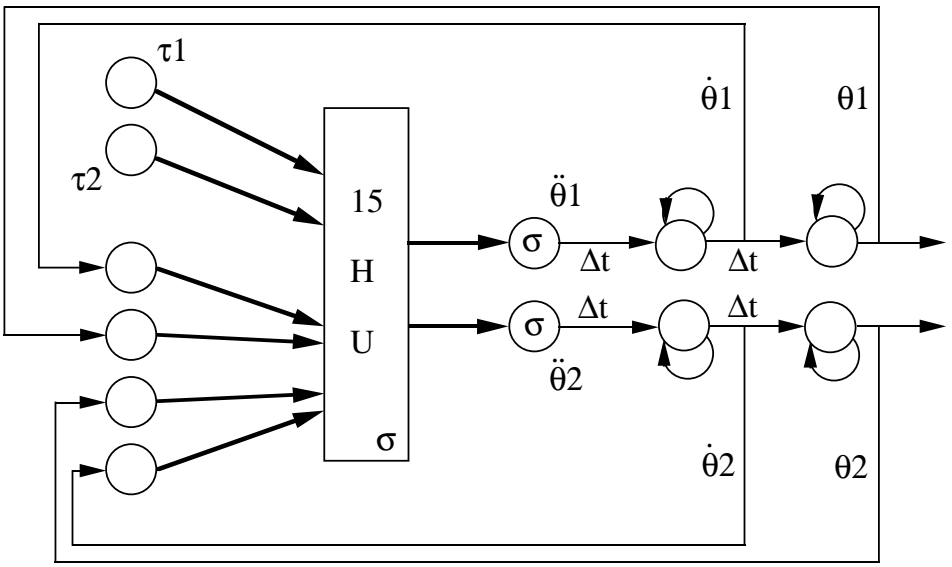

Figure 3: The recurrent network that was trained to implement the arm forward dynamics. Sigmoidal units are indicated with σ. All other units are linear. HU: hidden units.

integrators and the recurrent connections to the input layer, and the resulting imperfect values of angular positions and velocities are also fed back to the six muscle networks (see Figure 1), possibly amplifying the errors even more. It is then important to assess if the residual training errors are small enough to allow the arm to remain stable for a significant interval of time, or if instability occurs too soon. If the latter was the case, then the model would be quite inappropriate for our goals. It would be inappropriate for studying which features of the movements can be attributed to the plant properties alone because with an unstable system it would be hard to distinguish between aspects of movements due to the effects of the neural input and aspects of movements due instead to natural drifting. The model would also be inappropriate for future motor learning studies because an eventual controller would be forced to compensate for the inherent instability of the plant hindering its real control functions. The response of the system to equilibrium levels of neural input is shown in Figures 4 and 5.

The arm remained steady at its initial posture for approximately 410 time steps (the first 400 are shown in Figure 4), i.e., for 2.05 *sec.*, after which the endpoint began to drift slowly towards the bottom left portion of the workspace. We considered this steady-state response satisfactory from the standpoint of the two goals of our study, because it provided us with an initial 2 *sec.* window during which the movements of the arm were clearly due to the patterns

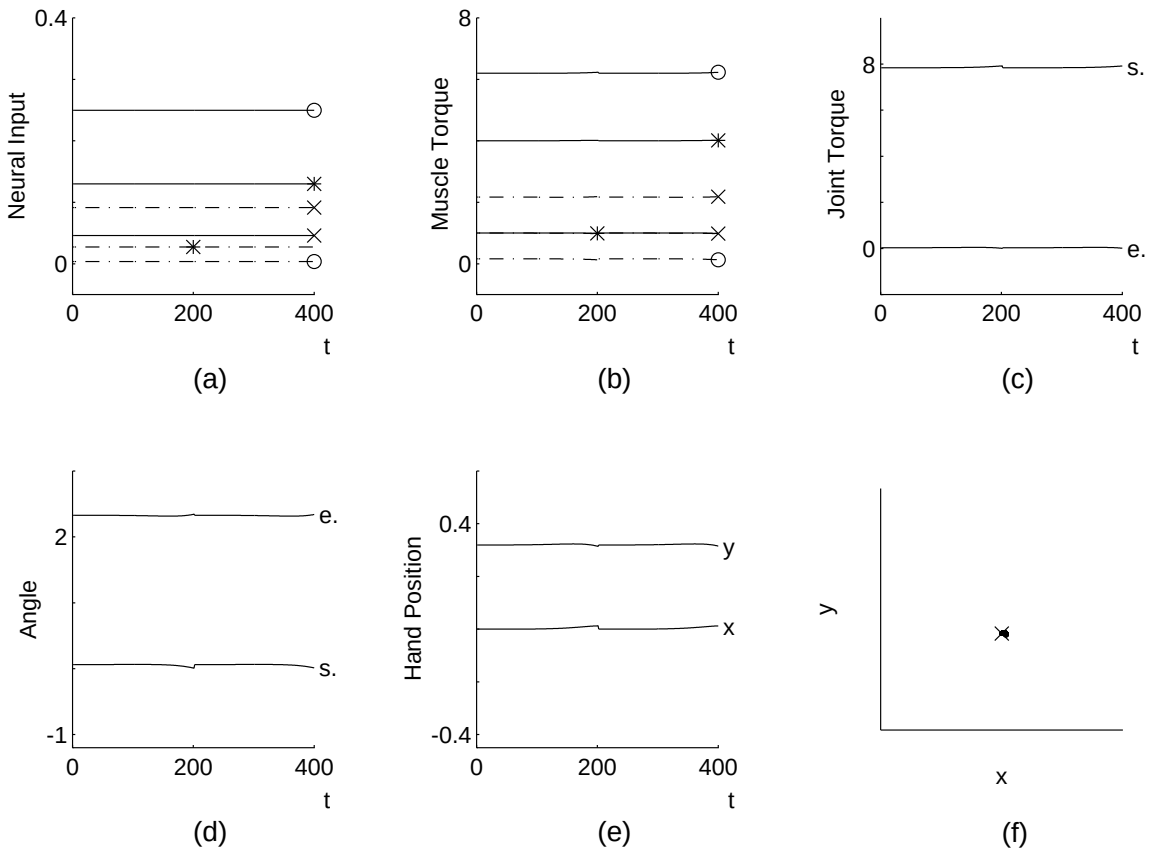

Figure 4: Stability test, time steps 0 to 400. One time step = 5 *msec.* In (a) and (b): open circles = shoulder muscles, cross = elbow muscles, asterisk = double-joint muscles, solid line = flexor, dotted line = extensor. The terms "flexor" and "extensor" are used throughout this paper to indicate muscles that move the arm towards the body and away from the body respectively. In (f) the cross indicates the position of the arm endpoint at $t = 0$, the dots on the cross indicate the actual trajectory of the endpoint during 400 time steps.

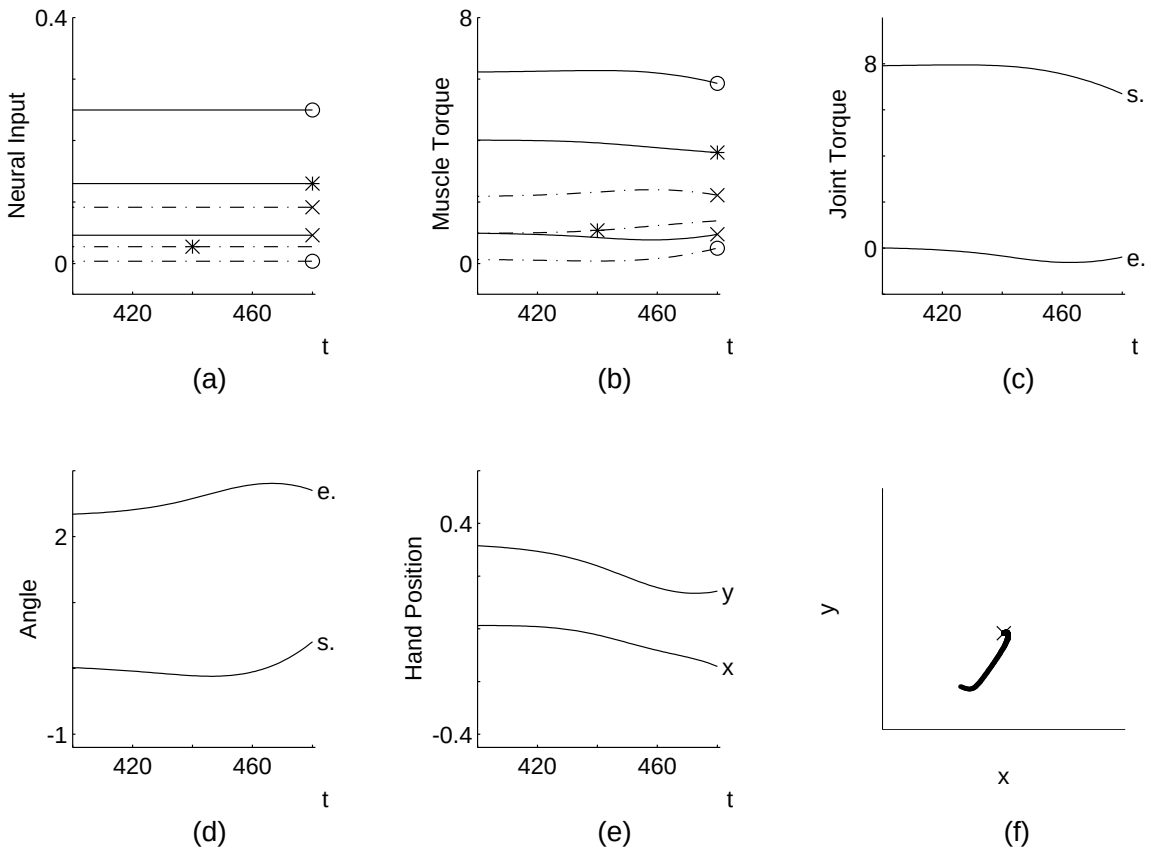

Figure 5: Stability test, time steps 400 to 480. After 100 time steps the arm endpoint begins to drift towards the bottom left area of the workspace.

of neural input and not to instability phenomena.

2.2 General Considerations

The simulation results that follow demonstrate what types of movements the model produces when the arm muscles are activated with simple patterns of neural input. It is important to point out that in all the simulations presented in this paper the arm model operates without a controller and that the modeled arm is a highly redundant device (six degrees of freedom in muscle space, two degrees of freedom in endpoint space.) Furthermore, each of the six neural inputs can exhibit arbitrary time-varying amplitude and arbitrary duration. Consequently it is impossible to predict which movements will result when randomly-selected profiles of neural input are applied. Hence the purpose of the simulations presented in the next subsection is not that of reproducing specific movements or having the arm endpoint reach certain specified locations of the workspace[1] – hardly achievable tasks in absence of a controller, but rather that of observing the macroscopic properties of the resulting (unpredictable) motor patterns. We must also point out that whenever the system is activated with some patterns of neural input, the response of the recurrent network that implements the forward dynamics of the arm is a generalization of that network to novel values of joint torques, angular velocities and angular positions. We do not know, in fact, which combination of neural inputs would produce the torque, velocity and angle profiles that we utilized to train the network. We are actually not even attempting to find that out, as previously emphasized. Hence the only situation where the forward dynamic network operates with known values of torque, position and velocity is when the neural inputs are at their equilibrium values (Figures 2b, 4 and 5.) Finally we would also like to point out that the overall system is highly nonlinear in many respects. First, the forward dynamic transformation is a highly nonlinear one. Second, the nonlinearity of the forward dynamic transformation propagates also to the muscle networks: Although we modeled the muscles as linear elastic devices, all muscle networks receive recurrent connections from the downstream units that represent joint positions and velocities (see Figure 1). These recurrent connections introduce a nonlinear component in the muscle networks. The third source of nonlinearity is the presence in the model of double-joint muscles. Because of their action, there is coupling in the model between the two arm links not only at the level of the forward dynamics, but also at the muscle level. Finally the forward kinematics is also a nonlinear transformation.

2.3 Step Response

Figures 6 to 13 illustrate the response of the model to the following stimulation paradigm: (i) One of the six muscles was activated with a step of neural input. The amplitude of the step was chosen randomly and its duration was arbitrarily set, for all movements within this paradigm, to 60 time steps (300 *msec.*). (ii) The opponent muscle was deactivated by setting its neural input to zero. (iii) The neural inputs for the remaining four muscles were maintained at their equilibrium levels. The 60-time-steps duration for the neural inputs was chosen a priori, i.e., independently of the actual outcome. Hence in some instances this choice led to complete movements, i.e., movements that ended with velocities close to zero, while in other instances it led to portions of movements. Figures 6 and 7 show the results of activating the elbow flexor. Figure 6a shows the patterns of neural input for the muscle that was activated

[1] These control problems have been addressed in a number of previous works (including works by one of the authors of this paper), e.g., [6], [7], [9], [10], [11], [12], [13].

(elbow flexor) and the muscle that was deactivated (elbow extensor). The neural inputs for the remaining four muscles (not shown in Figure 6a) were maintained at their equilibrium level (Figure 2b). Figures 6b, 6c, 6d, 6e illustrate respectively the resulting profiles of muscle torque ($N \cdot m$), joint torque ($N \cdot m$), joint angles (rad) and endpoint coordinates. Figure 6f shows the resulting motion of the endpoint. Figure 7a and 7b show the angular velocities

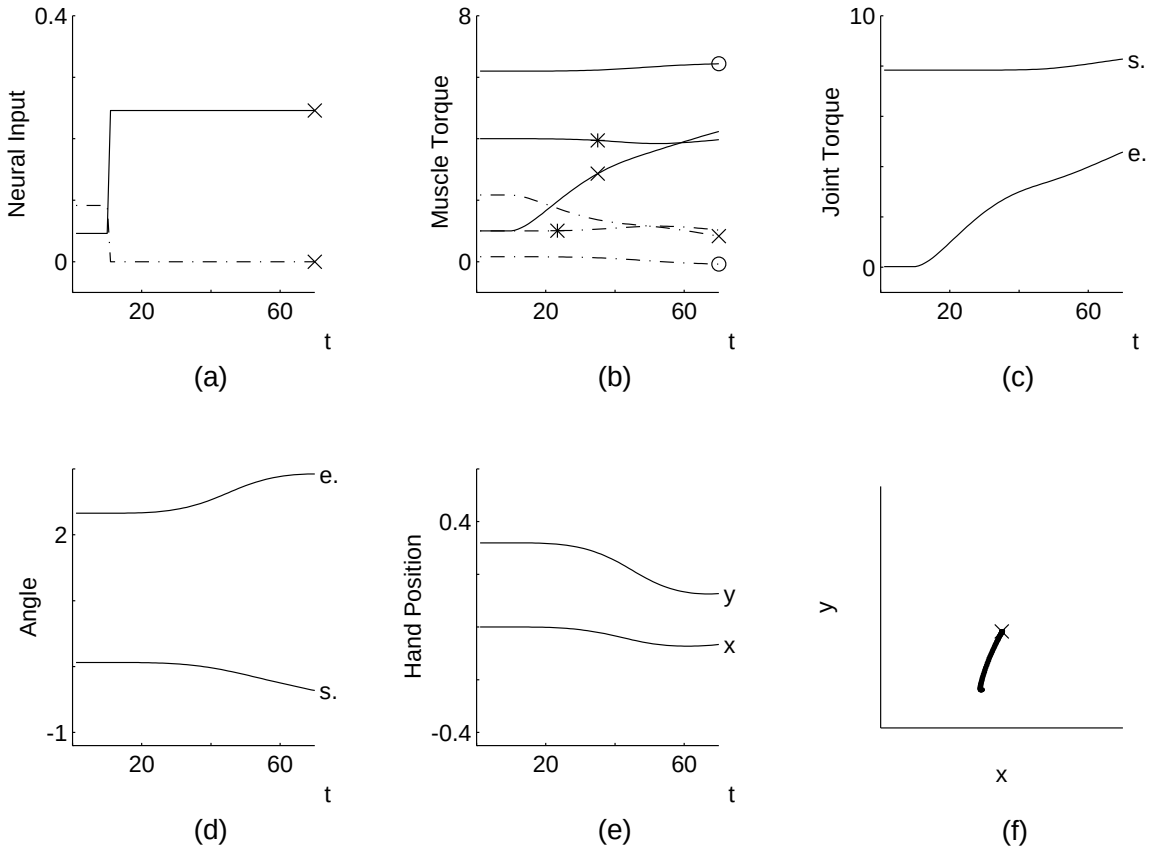

Figure 6: Response of the model to activation of the elbow flexor and deactivation of the elbow extensor.

(rad/sec) and the angular accelerations (rad/sec^2) as they are computed by the forward-dynamics network. Figures 7c and 7d show respectively the horizontal and vertical velocities of the endpoint (m/sec) and the endpoint velocity along the path. Figures 7e and 7f show instead the acceleration of the endpoint (m/sec^2), again along the two axes and along the endpoint path, respectively. We computed the horizontal and vertical velocities ($\dot{x}, \dot{y}$) and accelerations ($\ddot{x}, \ddot{y}$) of the endpoint analytically by taking the first and second derivatives of the forward kinematics equations

$$x = \ell_1 \cos\theta_1 + \ell_2 \cos(\theta_1 + \theta_2) \tag{1}$$

$$y = \ell_1 \sin\theta_1 + \ell_2 \sin(\theta_1 + \theta_2) \tag{2}$$

and by substituting in the resulting equations the values of $\theta, \dot{\theta}$, and $\ddot{\theta}$ computed by the forward-dynamics network. We then computed the endpoint velocity, v, and acceleration, a, along the path as

$$v = (\dot{x}^2 + \dot{y}^2)^{1/2} \tag{3}$$

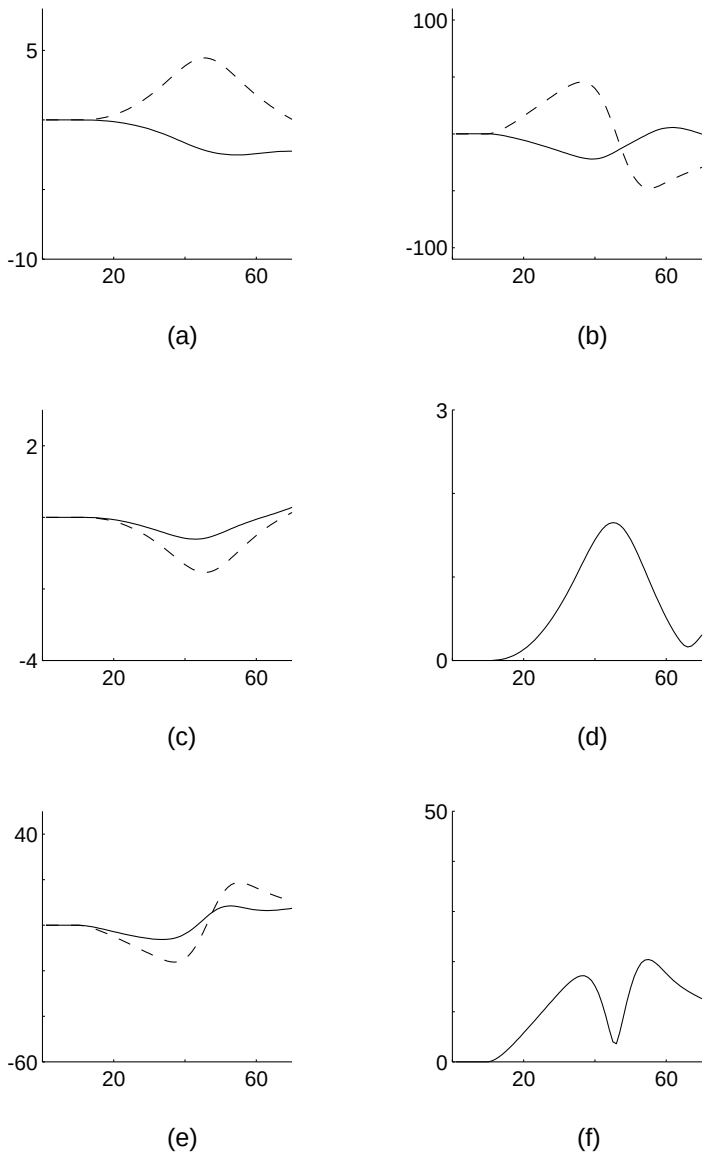

Figure 7: Velocities and accelerations for the movement shown in Figure 6(f). (a) Joint velocities computed by the forward-dynamics network. Solid line: shoulder joint. Dotted line: elbow joint. (b) Joint accelerations computed by the forward-dynamics network. Solid line: shoulder joint. Dotted line: elbow joint. (c) Horizontal (solid line) and vertical (dotted line) velocities of the endpoint. (d) Endpoint velocity along the path. (e) Horizontal (solid line) and vertical (dotted line) accelerations of the endpoint. (f) Endpoint acceleration along the path.

$$a = (\ddot{x}^2 + \ddot{y}^2)^{1/2} \tag{4}$$

The acceleration, a, is hence, in our figures, the rectified derivative of v. When observing Figures 6 and 7, one immediately notices two things: (1) The resulting movement of the endpoint is "smooth," in the sense that it exhibits velocity and acceleration profiles free from discontinuities. (2) The endpoint velocity profile (Figure 7d) is unimodal and bell-shaped. Both features – smoothness of the path and bell-shapedness of the velocity profile – are distinctive features of arm movements executed by humans, primates and even lower species [14], [15]. The significance of these results will be discussed in Section 3. In the remainder of this section we further demonstrate the response of our model. Figures 8 and 9 show how the model responds to activation of the shoulder flexor and deactivation of the shoulder extensor. The interpretation of Figures 8 and 9 (and of all the figures that follow) is analogous to the

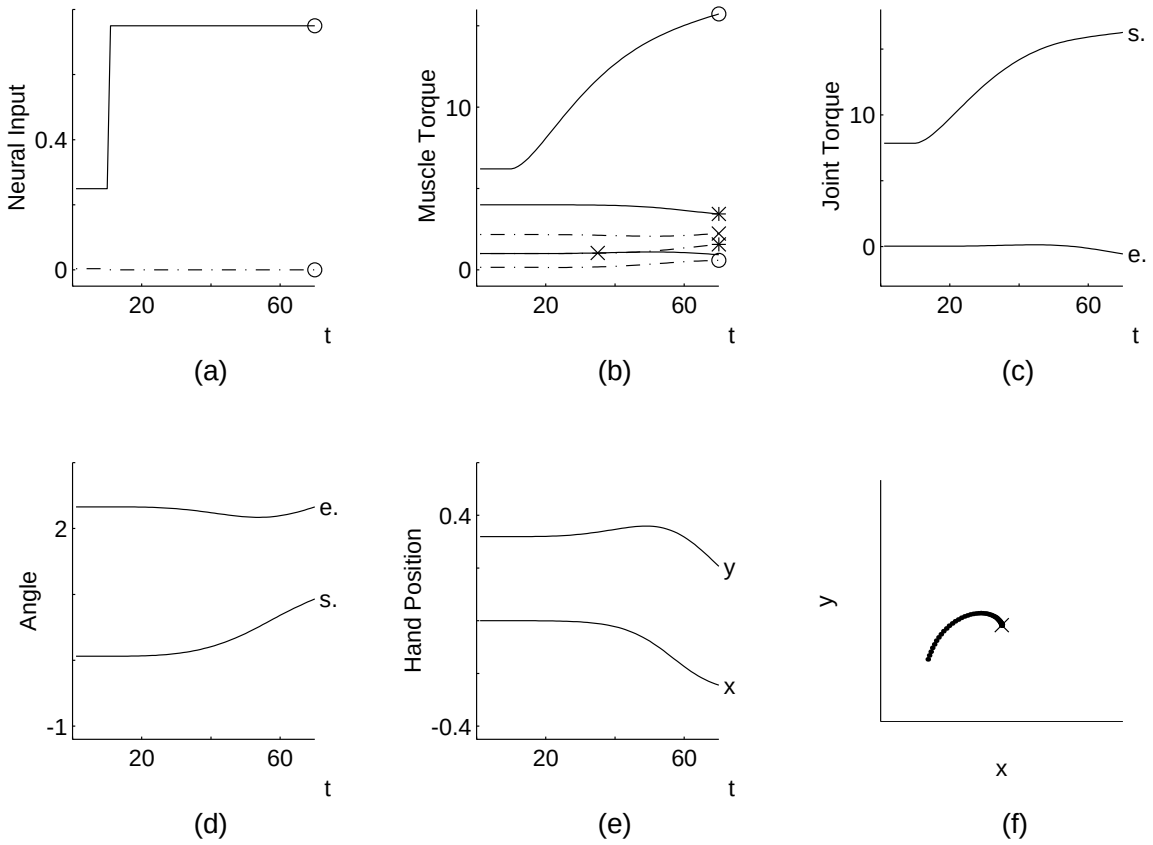

Figure 8: Response of the model to activation of the shoulder flexor and deactivation of the shoulder extensor.

interpretation of Figures 6 and 7. Figures 10 and 11 refer to activation of the double-joint extensor and deactivation of the double-joint flexor, while Figures 12 and 13 refer instead to the opposite task: activation of the double-joint flexor and deactivation of the double-joint extensor. In all these cases we could consistently observe smooth endpoint paths and unimodal velocity profiles.

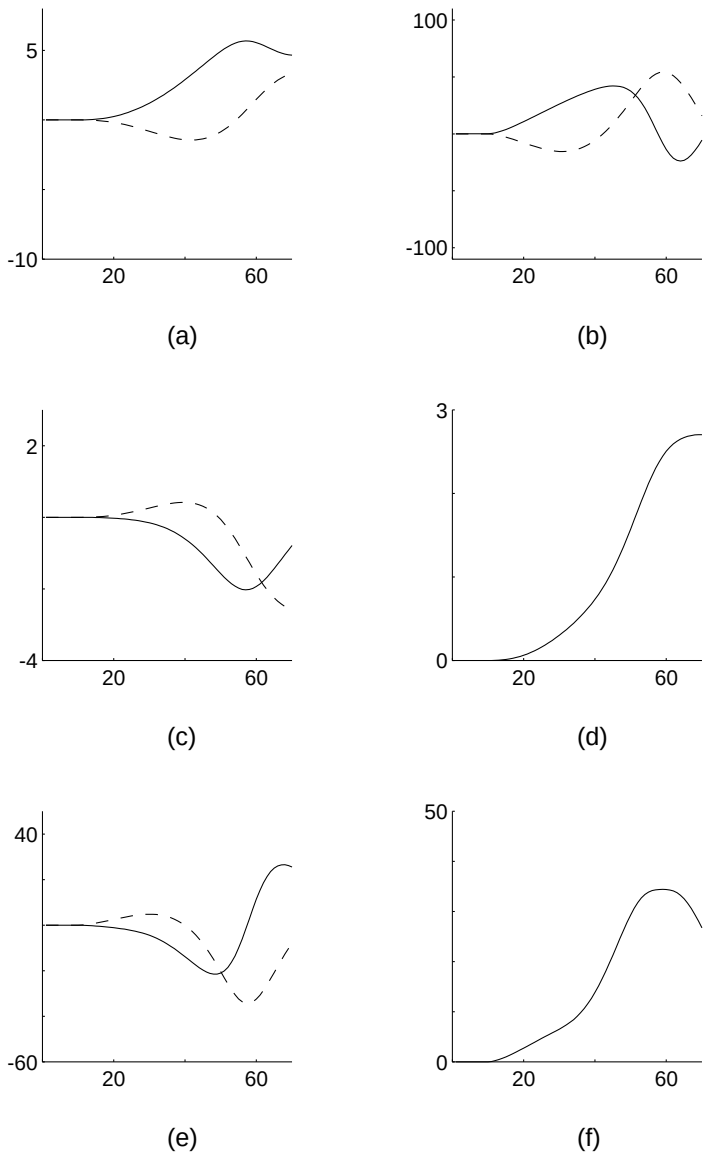

Figure 9: Velocities and accelerations for the movement shown in Figure 8(f). (a) Joint velocities computed by the forward-dynamics network. Solid line: shoulder joint. Dotted line: elbow joint. (b) Joint accelerations computed by the forward-dynamics network. Solid line: shoulder joint. Dotted line: elbow joint. (c) Horizontal (solid line) and vertical (dotted line) velocities of the endpoint. (d) Endpoint velocity along the path. (e) Horizontal (solid line) and vertical (dotted line) accelerations of the endpoint. (f) Endpoint acceleration along the path.

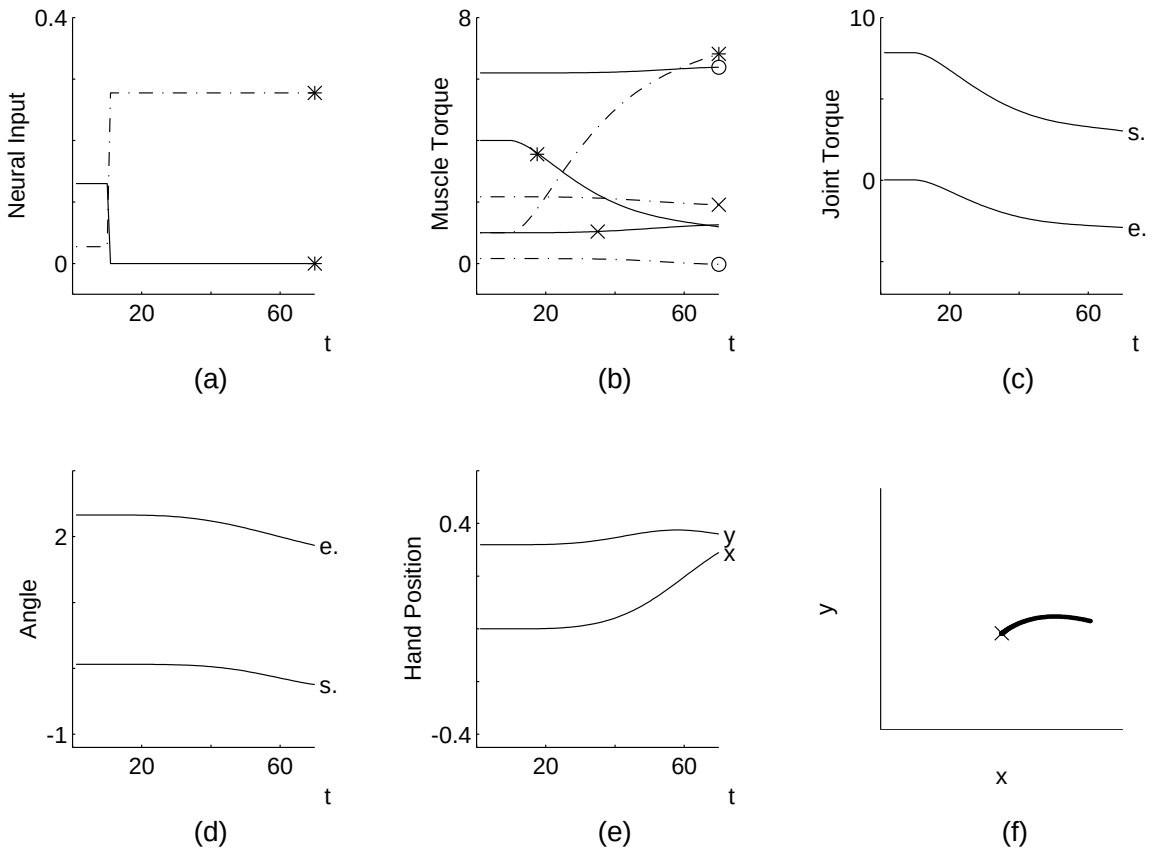

Figure 10: Response of the model to activation of the double-joint flexor and deactivation of the double-joint extensor.

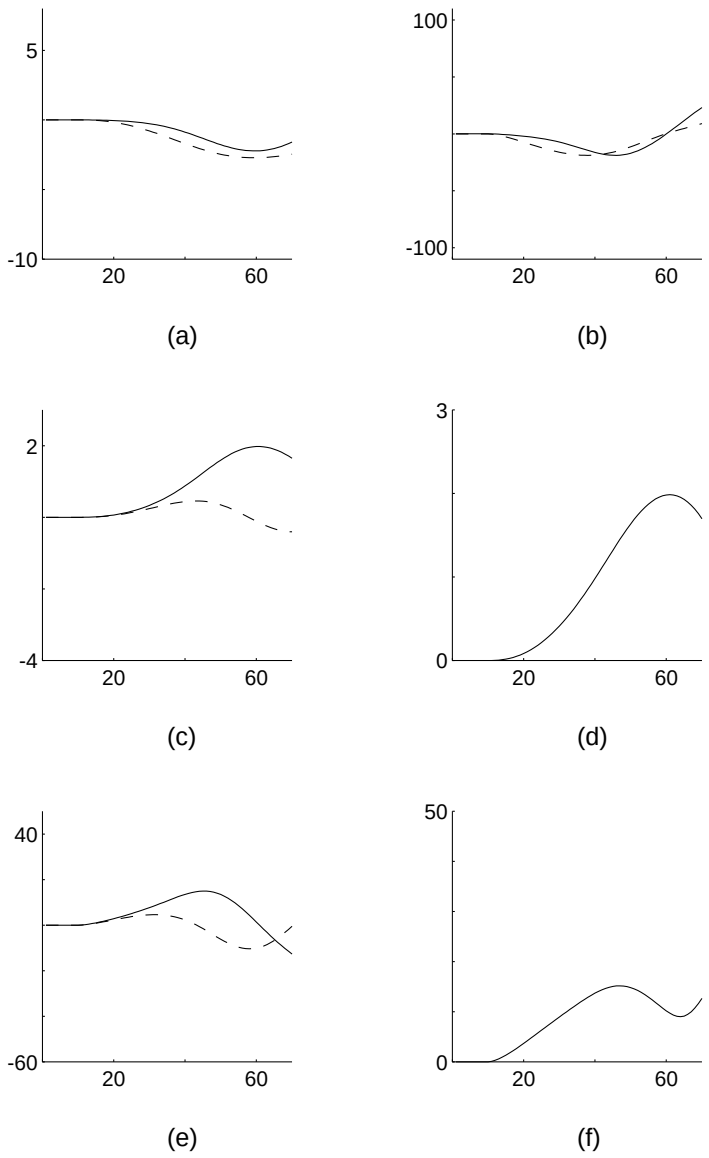

Figure 11: Velocities and accelerations for the movement shown in Figure 10(f). (a) Joint velocities computed by the forward-dynamics network. Solid line: shoulder joint. Dotted line: elbow joint. (b) Joint accelerations computed by the forward-dynamics network. Solid line: shoulder joint. Dotted line: elbow joint. (c) Horizontal (solid line) and vertical (dotted line) velocities of the endpoint. (d) Endpoint velocity along the path. (e) Horizontal (solid line) and vertical (dotted line) accelerations of the endpoint. (f) Endpoint acceleration along the path.

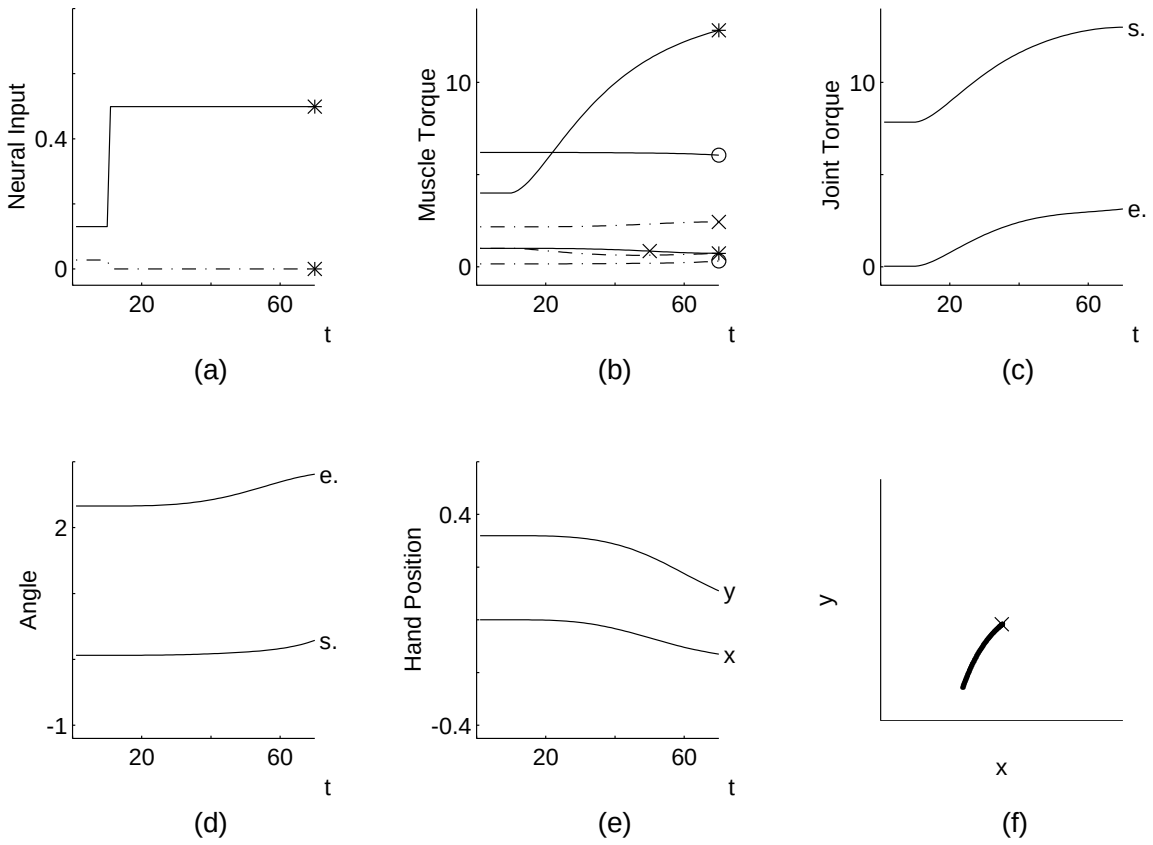

Figure 12: Response of the model to activation of the double-joint extensor and deactivation of the double-joint flexor.

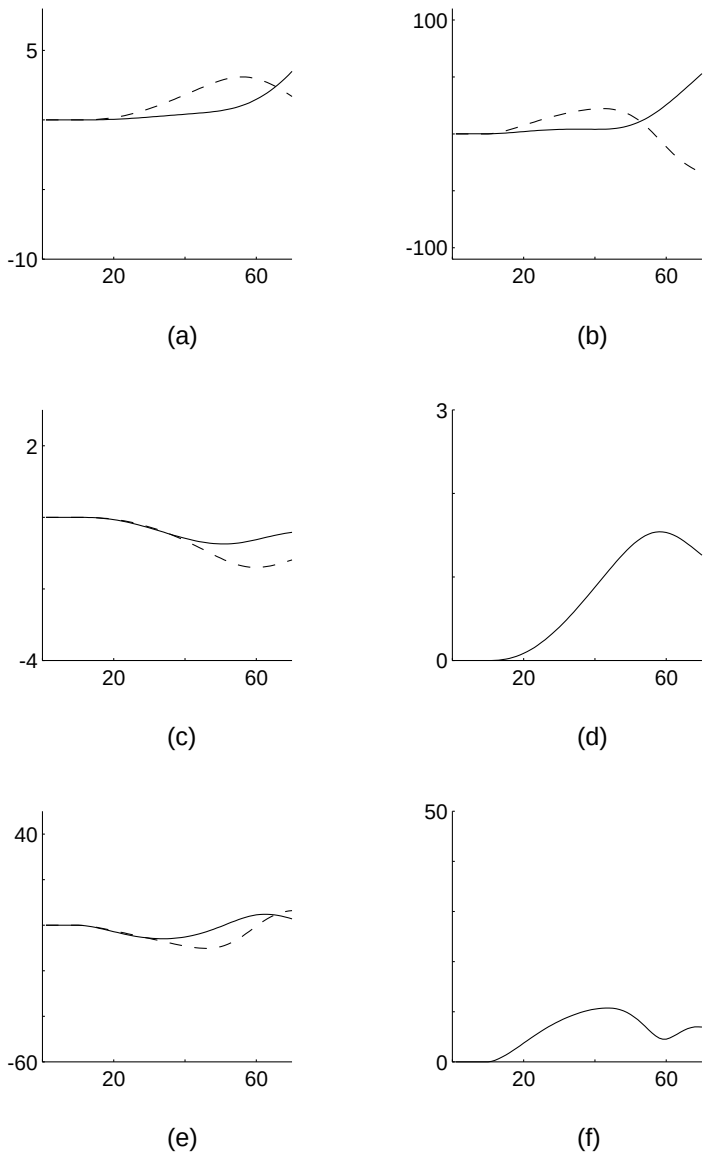

Figure 13: Velocities and accelerations for the movement shown in Figure 12(f). (a) Joint velocities computed by the forward-dynamics network. Solid line: shoulder joint. Dotted line: elbow joint. (b) Joint accelerations computed by the forward-dynamics network. Solid line: shoulder joint. Dotted line: elbow joint. (c) Horizontal (solid line) and vertical (dotted line) velocities of the endpoint. (d) Endpoint velocity along the path. (e) Horizontal (solid line) and vertical (dotted line) accelerations of the endpoint. (f) Endpoint acceleration along the path.

2.4 Step-Reversal Response

Figures 14 to 19 illustrate the response of the model to the following stimulation paradigm: (i) One of the six muscles was activated with a step of neural input of limited duration. (ii) The opponent was deactivated by setting its neural input to zero. (iii) At the end of the step, the active muscle was deactivated and its opponent activated with another step of limited duration. (iv) The neural inputs for the remaining four muscles were maintained at their equilibrium levels. Again the amplitudes of the two steps were chosen randomly, and their duration arbitrarily set, this time, to 50 steps each (250 *msec.*) independently of the outcome. The purpose of this experiment was to demonstrate what our model does when the activation of two antagonist muscles is suddenly reversed. Experimental studies of this kind executed with human subjects and/or primates report that when opposite groups of muscles are activated/deactivated, the endpoint reverses its direction of movement in a smooth fashion and the velocity profile has a tendency to be unimodal and bell-shaped in each portion of the path [16]. Figures 14 and 15 illustrate this experiment with the elbow muscles, Figures 16

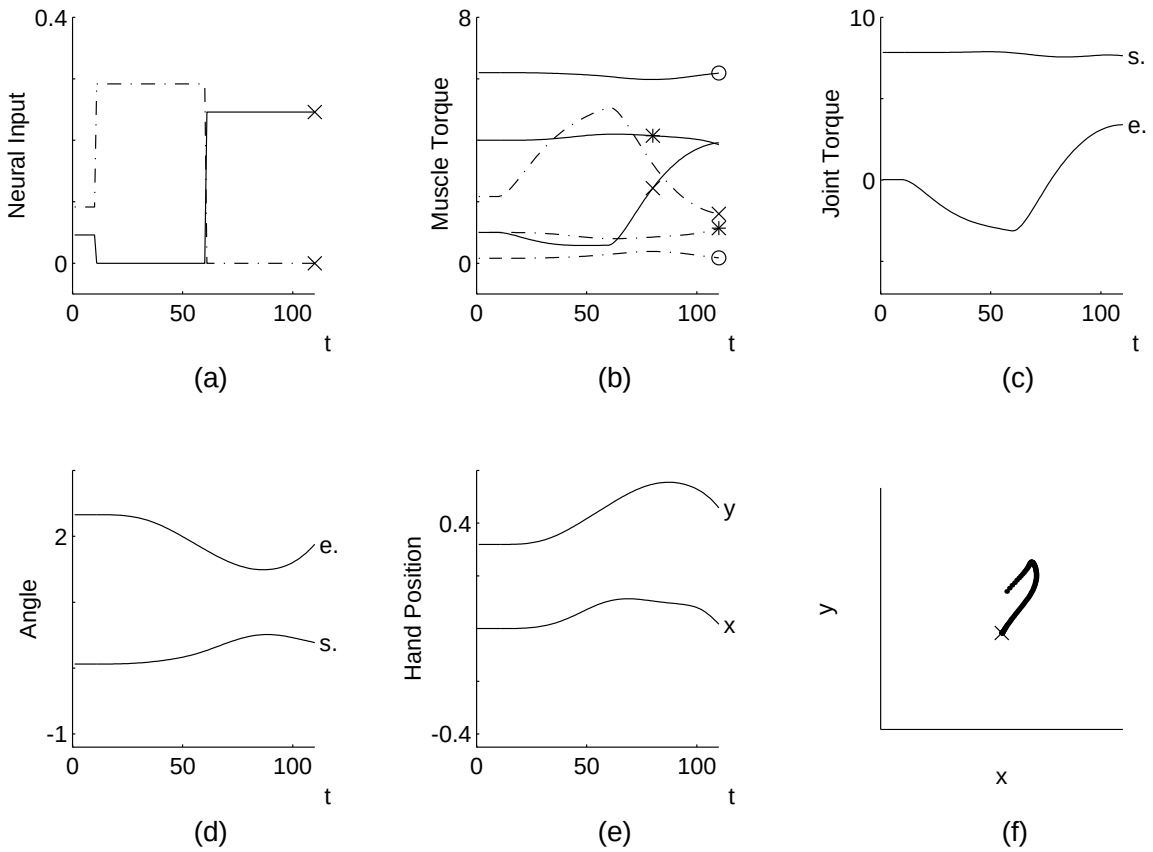

Figure 14: Response of the model to a step-reversal of the elbow muscles.

through 19 with the double-joint muscles. Observation of the resulting endpoint velocity and acceleration profiles shows a close match with the experimental data.

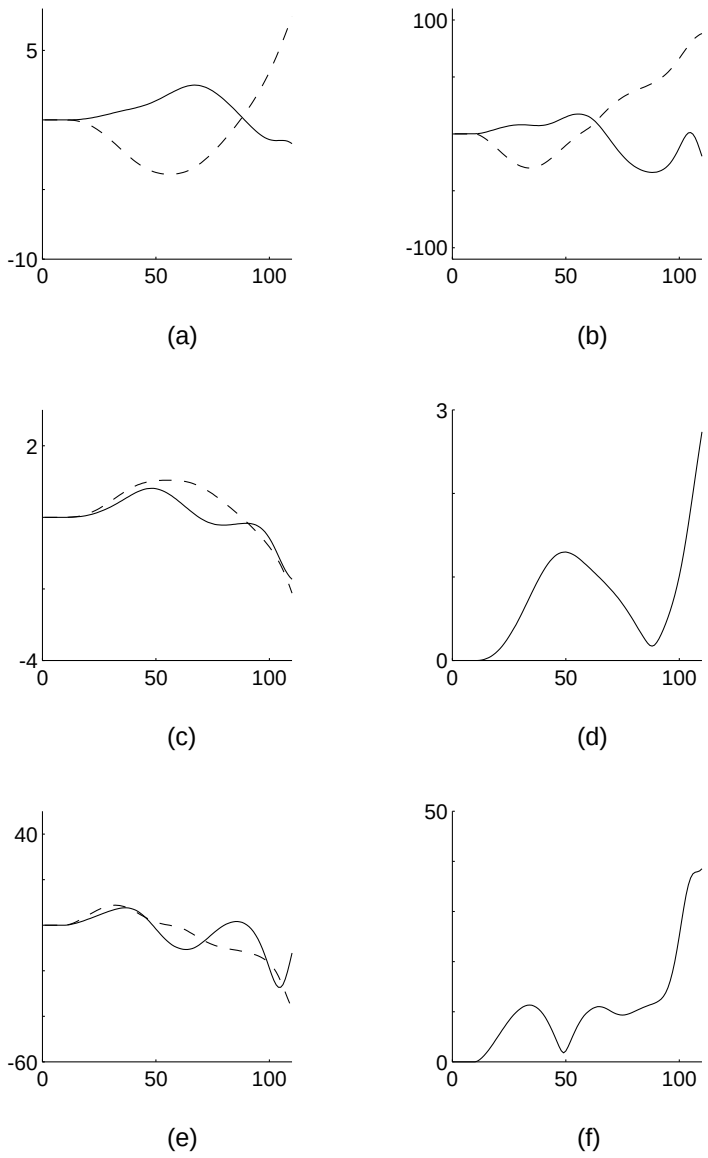

Figure 15: Velocities and accelerations for the movement shown in Figure 14(f). (a) Joint velocities computed by the forward-dynamics network. Solid line: shoulder joint. Dotted line: elbow joint. (b) Joint accelerations computed by the forward-dynamics network. Solid line: shoulder joint. Dotted line: elbow joint. (c) Horizontal (solid line) and vertical (dotted line) velocities of the endpoint. (d) Endpoint velocity along the path. (e) Horizontal (solid line) and vertical (dotted line) accelerations of the endpoint. (f) Endpoint acceleration along the path.

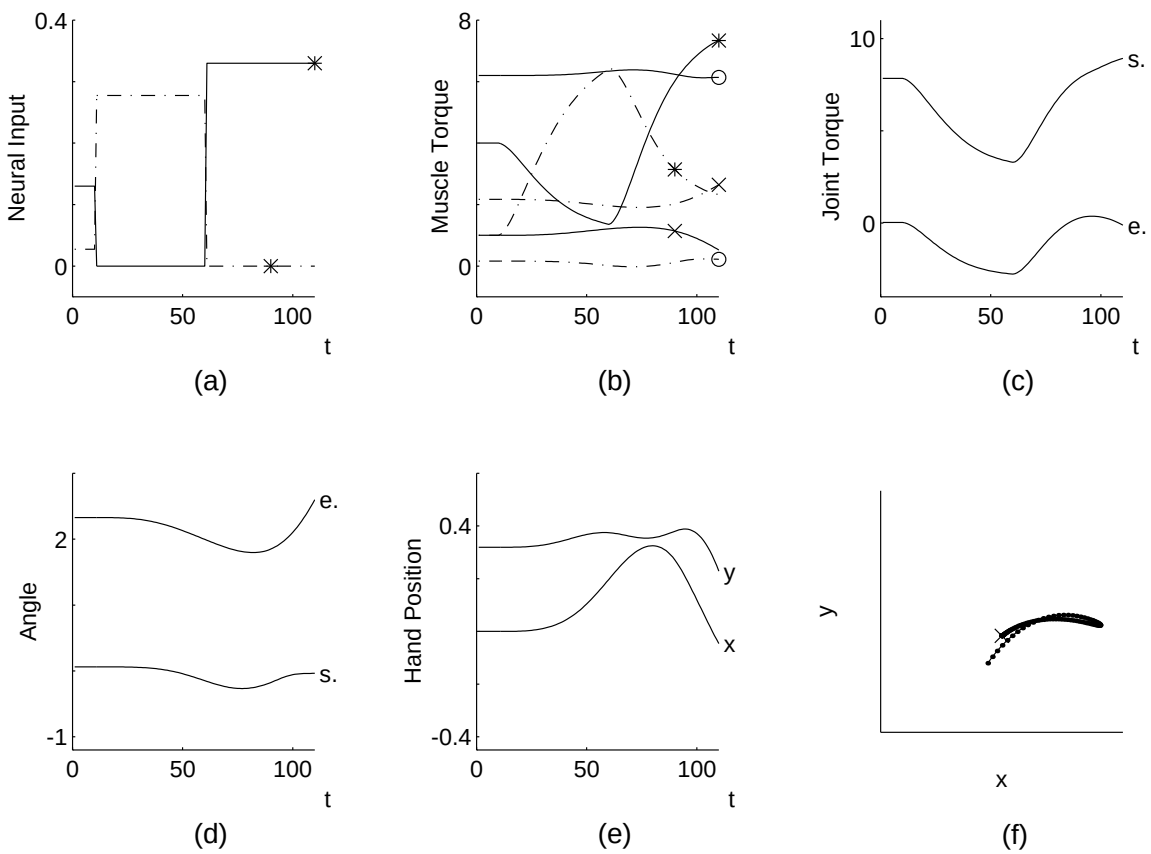

Figure 16: Response of the model to a step-reversal of the double-joint muscles.

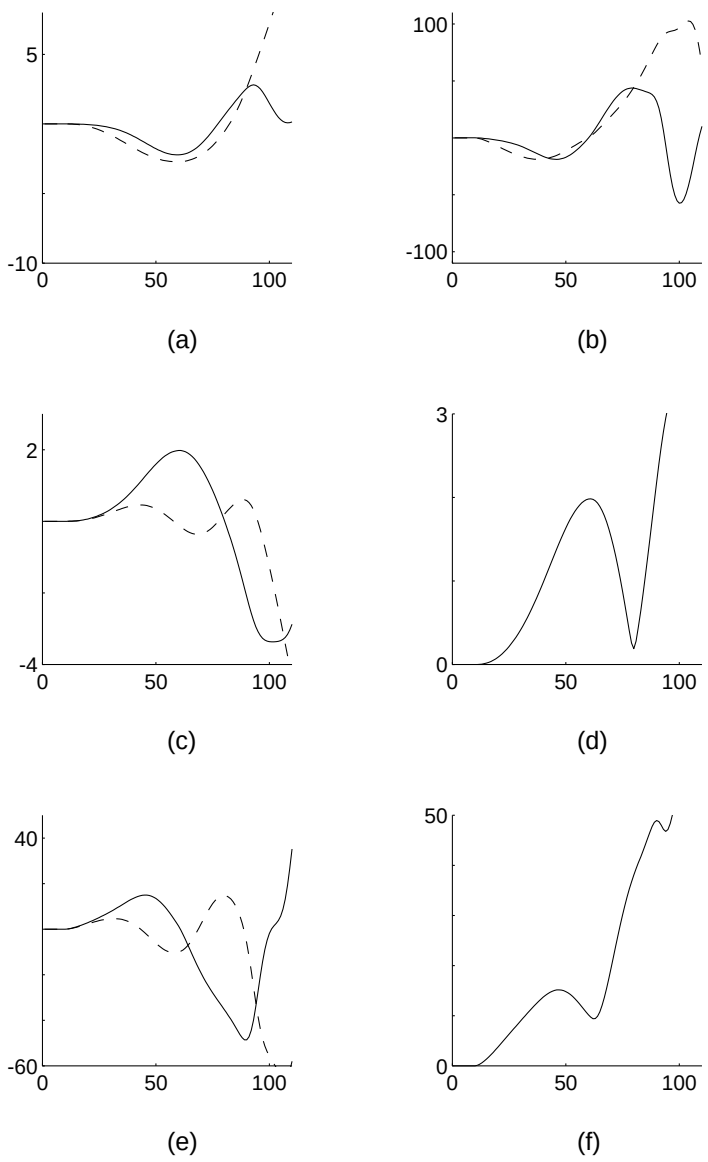

Figure 17: Velocities and accelerations for the movement shown in Figure 16(f). (a) Joint velocities computed by the forward-dynamics network. Solid line: shoulder joint. Dotted line: elbow joint. (b) Joint accelerations computed by the forward-dynamics network. Solid line: shoulder joint. Dotted line: elbow joint. (c) Horizontal (solid line) and vertical (dotted line) velocities of the endpoint. (d) Endpoint velocity along the path. (e) Horizontal (solid line) and vertical (dotted line) accelerations of the endpoint. (f) Endpoint acceleration along the path.

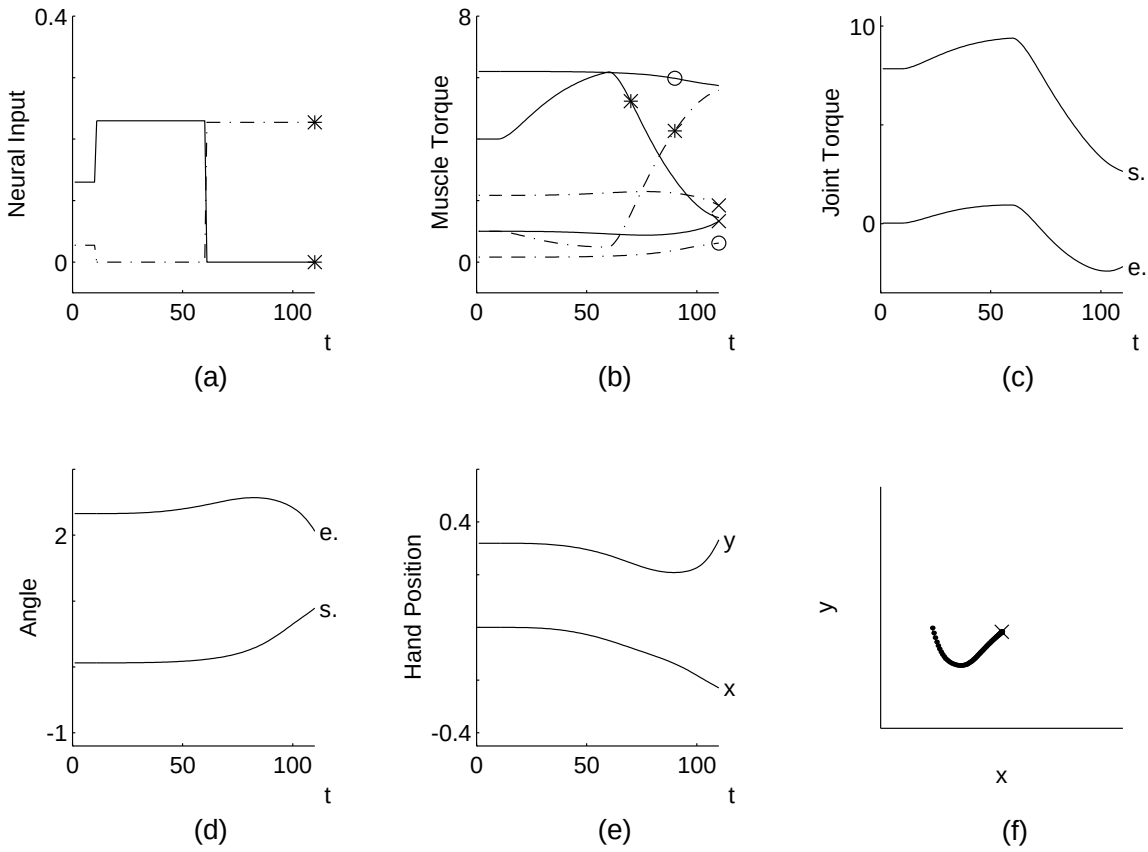

Figure 18: Response of the model to a step-reversal of the double-joint muscles.

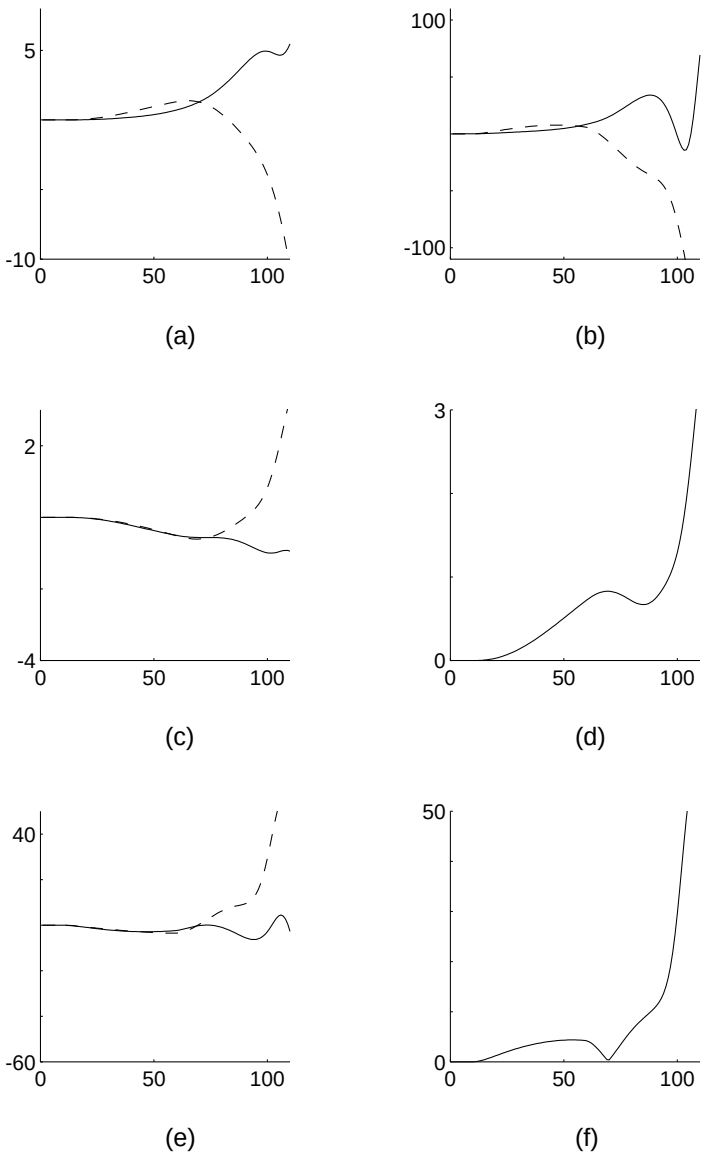

Figure 19: Velocities and accelerations for the movement shown in Figure 18(f). (a) Joint velocities computed by the forward-dynamics network. Solid line: shoulder joint. Dotted line: elbow joint. (b) Joint accelerations computed by the forward-dynamics network. Solid line: shoulder joint. Dotted line: elbow joint. (c) Horizontal (solid line) and vertical (dotted line) velocities of the endpoint. (d) Endpoint velocity along the path. (e) Horizontal (solid line) and vertical (dotted line) accelerations of the endpoint. (f) Endpoint acceleration along the path.

2.5 Multi-Step Response

In this final experiment we illustrate the response of our model to a sequence of random and intermixed activations/deactivations of the six muscles (Figures 20 and 21). The resulting movement of the endpoint (Figure 20f) is composed of two tracts that are practically straight

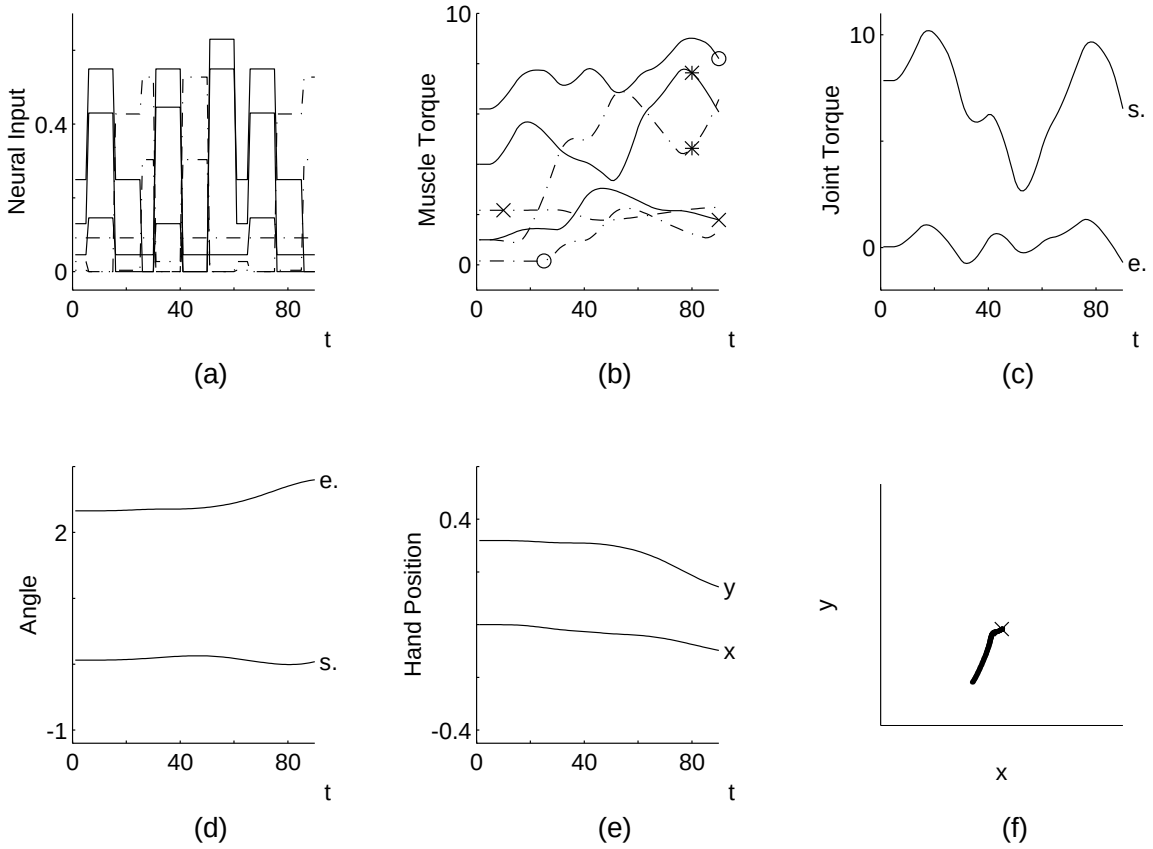

Figure 20: Response of the model to sequence of random intermixed activations of all the muscles.

(an initial short tract followed by a longer one). Despite the randomness of the neural inputs, the two distinctive features – smoothness of the path and unimodal, bell-shaped velocity profiles – are still in place for each tract (see Figure 21d).

3 Discussion

3.1 Results

In this paper we demonstrated the response of a neural-network model of a planar redundant arm (whose structure and operation principles were inspired by those of the human arm) to various patterns of activation of its muscles. The motivation for choosing the human arm as a reference was the observation that the properties of the human arm, particularly the elastic properties of muscles, are likely to be an important component of the human ability to exhibit dexterous skilled behavior – a kind of behavior yet to be achieved with artificial arms. In the first simulation experiment (Figures 4 and 5) we demonstrated the

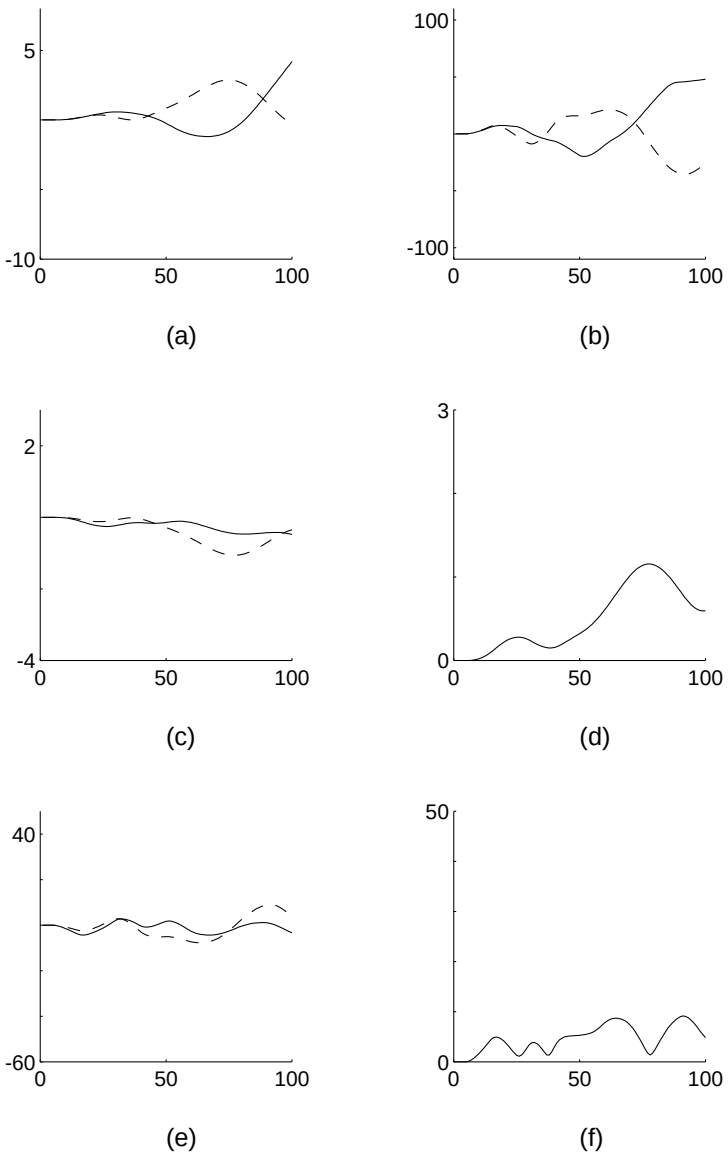

Figure 21: Velocities and accelerations for the movement shown in Figure 20(f). (a) Joint velocities computed by the forward-dynamics network. Solid line: shoulder joint. Dotted line: elbow joint. (b) Joint accelerations computed by the forward-dynamics network. Solid line: shoulder joint. Dotted line: elbow joint. (c) Horizontal (solid line) and vertical (dotted line) velocities of the endpoint. (d) Endpoint velocity along the path. (e) Horizontal (solid line) and vertical (dotted line) accelerations of the endpoint. (f) Endpoint acceleration along the path.

stability of our model by activating the muscles with constant neural inputs at their computed equilibrium levels. This successful test was important to assess the robustness of the model to errors, the generalization abilities of the forward dynamic network in the vicinity of the initial arm posture and the overall adequacy of the model for further analyses. Once stability was established, we activated our model with three types of patterns, that we called step, step-reversal and multi-step respectively. In each case we analyzed the global kinematic properties of the resulting movements of the arm endpoint. Such movements are unpredictable because of the redundancy of the arm. We quite consistently (and in many more instances than presented in this paper) found that the movements of the endpoint were "smooth" in the sense that the endpoint velocities and accelerations were free from discontinuities. In addition, the endpoint velocity profiles along the path had a clear tendency to be unimodal and in many cases exactly bell-shaped. Furthermore, with the step-reversal stimulation paradigm, the endpoint reversed its direction of movement smoothly, without exhibiting discontinuities in neither its path, nor its velocity, nor its acceleration. The velocity along these paths was also characterized by two peaks, one for every portion of the path. Smoothness, unimodal velocity profiles, and smooth reversal of the direction of movement are properties consistently found in arm movements executed by humans, primates and even lower species. Morasso [14], for example, recorded the velocity profiles of point-to-point movements executed by human subjects in a variety of conditions. His recordings showed that while there was variability in the profiles of the joint velocities, the endpoint velocity profiles were consistently bell-shaped. Flash and Hogan [15] demonstrated that a minimum-jerk[2] model fits well the paths and velocity profiles of point-to-point movements. This result implies that such movements exhibit smooth velocity and acceleration profiles. Georgopoulos et al. [16] experimented with primates trained to move their hand in the direction of a flashing target. When targets were switched so as to cause a reversal of the direction of movement of the hand, the resulting hand paths were globally smooth and exhibited bell-shaped velocity profiles in each tract. We were able to reproduce all of these findings by activating our arm model with random steps of neural input. We interpret our results as an indication that the properties of the plant play a significant role in trajectory formation, and that some of the basic kinematic aspects of movements are dictated by such properties. These results are significant in many respects. From an engineering perspective they seem to indicate that the task of an eventual controller could simply be that of selecting appropriate amplitudes and durations for the neural inputs without considering additional motor details. Hence our results tell us that it is important that artificial arms are built according to biological principles because the resulting movements will exhibit smoothness and unimodal velocity profiles in response to very simple step-like patterns of activation and that such arms will require simple controllers in order to operate. One could also interpret our results as relevant to the problem of understanding what strategies the central nervous system utilizes in order to control movements of the arms – the biological perspective. However, we must point out that our model is not a faithful reproduction of a human arm, but rather a model inspired by the properties of the latter. A human arm is, in fact, characterized by muscles that are nonlinear elastic elements, and their nonlinearities are likely to play some role. In our work we chose to represent the muscles as linear devices in order to keep the model to a manageable level of complexity but also because it was our desire to produce results relevant to the engineering of artificial arms. From this latter perspective it is important to demonstrate what linear actuators can actually do. Despite the linearity of the muscles in our model, we believe that our results can provide some ground for further investigations into the

[2] Jerk is defined as the time derivative of acceleration.

biological system. Should the present model be modified to represent the nonlinearities of the muscles, then one could compare the responses of the two models and gain some insights into what the role of muscles nonlinearities in trajectory formation might be. We are planning to modify our model to include nonlinear actuators in the near future. Such a modification would imply the use of learning techniques also for the muscle networks. We must however recall that Oguztoreli and Stein [5] experimented with both a linear and a nonlinear model of muscles that executed single-joint movements of the wrist, and they found that, although the nonlinearities of the muscles added some complexity to the computation and were important to the mechanisms of force generation, they did not qualitatively change the overall control of movement. This has, however, yet to be proven in the multijoint case.

In future research we will also address the arm control problem. We specifically chose to carry out this study without considering control aspects because we deemed important to asses first what our arm model could do on its own. Although there have been many modeling works that addressed the arm control problem (see footnote 1 and next subsection), to the best of our knowledge no analysis has been carried out so far of what types of movements result from a neural model of an arm when the arm muscles are randomly activated. The present research was meant to fill this gap.

3.2 Relationship to Other Modeling Work

Arm movements have been widely studied during the last two decades and from a variety of different perspectives. While a review of the vast arm-movement literature is clearly outside the scope of this paper, we would like to mention here two studies that are closely related to our research. Jordan et al. [6] presented a neural-network model of an arm. A comparison between Jordan et al.'s arm model and our arm model was carried out in [1]. In [6] Jordan et al. proposed also a method to control point-to-point movements of the arm in which a controller was learned using a set of via points. Their analysis of the resulting movements pointed out that such movements exhibited smoothness and bell-shaped velocity profiles. For single-joint movements, the authors argued that the plant properties were likely to be responsible for those effects and that control of amplitude and duration of the motor commands was indeed a sufficient, possible strategy. In the case of multijoint movements, however, Jordan et al. argued that an amplitude/duration control strategy alone would not be sufficient to obtain point-to-point movements with smooth straight paths and bell-shaped velocity profiles and that additional geometric and smoothing constraints were needed at the controller level. Our results seem to indicate that an amplitude/duration control strategy is, on the contrary, a possibility also for multijoint movements. Although we did not actually attempt to control the arm, i.e., we did not force the arm to follow straight paths towards a specified target, all the movements that we obtained following random activation of the muscles were smooth and their velocity profiles were unimodal. Furthermore, in a number of instances (see for example, Figures 6, 12, 14 and 21) the resulting paths, or portions thereof, were practically straight. There are differences between Jordan et al.'s arm model and our arm model as pointed out in [1], most notably the facts that their model does not contain double-joint muscles and does not represent the effects of gravity. It is hence possible that these differences, particularly the presence in our model of double-joint muscles, might be responsible for the different outcomes. We are currently further investigating this matter.

Katayama and Kawato [7] presented a computational model of a human arm with single and double-joint muscles. Their muscles were modeled according to the Kelvin-Voight model [17]. Katayama and Kawato utilized their arm model, together with a controller based

on the minimum-muscle-tension-change criterion [18], in order to predict, by computer simulation, virtual trajectories and stiffness ellipses during multijoint movements. The results of their simulation demonstrated that arm movements are so complex (even in their simple virtual-trajectory formulation [15]) that their control requires the presence of inverse models of the arm dynamics. Hence their work emphasizes, in a sense, the importance of the plant properties and the necessity of representing them internally in order to successfully control the arm. The work presented in this paper demonstrates that some of the well-known properties of human movements appear even in complete absence of a controller, when simple steps of neural input are applied. Hence our work builds additional support for Katayama and Kawato's statement that the plant properties are a crucial component of the arm motor system. This fact is important, as previously pointed out, from both an engineering and a biological perspective. From an engineering standpoint it shows that there is considerable advantage to designing artificial arms according to biological principles. From a biological perspective it stresses that, when trying to understand the link between behavior and neural mechanisms, one cannot ignore the properties of the circuitry in between.

Acknowledgements. This research was supported by the National Science Foundation, grant n. BCS-9113455 to Lina L.E. Massone. Thanks to Wynne Lee for her comments on the manuscript.

References

[1] L.L.E. Massone and J.D. Myers, "A neural network model of an anthropomorphic arm," *IEEE Trans. SMC*, submitted.

[2] A.V. Hill, "The heat of shortening and the dynamic constants of muscle," *Proc. Royal Society of London*, vol. B126, pp. 136-195, 1938.

[3] R.B. Stein, F.W.J. Cody and C. Capaday, "The trajectory of human wrist movements," *Journal of Neurophysiology*, vol. 59, pp. 1814-1830, 1988.

[4] M.N. Oguztoreli and R.B. Stein, "Optimal task performance of antagonistic muscles," *Biological Cybernetics*, vol. 64, pp. 87-94, 1990.

[5] M.N. Oguztoreli and R.B. Stein, "The effect of variable mechanical impedance on the control of antagonistic muscles," *Biological Cybernetics*, vol. 66, pp. 87-93, 1991.

[6] M.I. Jordan, T. Flash and Y. Arnon, "A model of the learning of arm trajectories from spatial deviations," *Journal of Cognitive Neuroscience*, in press.

[7] M. Katayama and M. Kawato, "Virtual trajectory and stiffness ellipse during multijoint arm movement predicted by neural inverse models," *Biological Cybernetics*, vol. 69, pp. 353-362, 1993.

[8] W.H. Zangemeister, S. Lehman and L. Stark, "Simulation of head movement trajectories: model and fit to the main sequence," *Biological Cybernetics*,vol. 41, pp. 19-32, 1981.

[9] L. Massone and E. Bizzi, "A neural network model for limb trajectory formation," *Biological Cybernetics*, vol. 61, pp. 417-425, 1989.

[10] L.L.E. Massone, "A biologically-inspired architecture for reactive motor control," in *Neural Networks in Robotics*, G.A. Bekey and K.Y. Goldberg, Eds., pp. 421-438. Boston: Kluwer Academic Publisher, 1993.

[11] Y. Wada and M. Kawato, "A neural network model for arm trajectory formation using forward and inverse dynamic models," *Neural Networks*, vol. 6, pp. 919-932, 1993.

[12] H. Gomi and M. Kawato, "Neural network control for a closed-loop system using feedback-error-learning," *Neural Networks*, vol. 6, pp. 933-946, 1993.

[13] M. Hirayama, M. Kawato and M.I. Jordan, "The cascade neural network model and a speed-accuracy trade-off of arm movement," *Journal of Motor Behavior*, vol. 25, pp. 162-174, 1993.

[14] P. Morasso, "Spatial control of arm movements," *Experimental Brain Research*, vol. 42, pp. 223-227, 1981.

[15] T. Flash and N. Hogan, "The coordination of arm movements: an experimentally confirmed mathematical model," *Journal of Neuroscience*, vol. 5, pp. 1688-1703, 1985.

[16] A.P. Georgopoulos, J.F. Kalaska, J.T. Massey, "Spatial trajectories and reaction times of aimed movements: effects of practice, uncertainty and change in target location," *Journal of Neurophysiology*, vol. 46, pp. 725-743, 1981.

[17] N. Ozkaya and M. Nordin, *Fundamental of biomechanics: equilibrium, motion and deformation*. New York: Van Nostrand Reynold, 1991.

[18] Y. Uno, R. Suzuki, M. Kawato, "Minimum muscle-tension-change model which reproduces human arm movements," *Proceedings of the 4th Symposium on Biological and Physiological Engineering*, pp. 299-302, 1989.